DOI: https://doi.org/10.37434/tpwj2025.09.05

INFLUENCE OF PULSE PLASMA TREATMENT ON WEAR RESISTANCE OF 40Kh STEEL SURFACE LAYERS

O.V. Kolisnichenko[1], V.M. Korzhyk[1], C. Senderowski[2], D.V. Strogonov[1], O.V. Hanushchak[1], O.S. Tereshchenko[1]

[1]E.O. Paton Electric Welding Institute of the NASU
11 Kazymyr Malevych Str., 03150, Kyiv, Ukraine
[2]Warsaw University of Technology, Mechanics and Printing Institute,
Narbutta 85, 02-524, Warszawa, Poland

ABSTRACT

The paper studies the effect of pulse plasma treatment on the physical and mechanical properties of 40Kh steel. The structural and phase changes were studied in the surface layers using metallographic and X-ray phase analysis. Cyclic action and high heating and cooling rates in the surface layers lead to a change in the kinetics of phase transformations, generation of inhomogeneous distortions of the crystal lattice as a result of phase strain hardening, a decrease in the dispersion of the structure, formation of an increased dislocation density, etc. Tribological tests for wear resistance were carried out under fluid friction conditions at various loads and sliding speeds. Comparative data on the extent of linear wear and wear intensity of the test samples were obtained.

KEYWORDS: pulse plasma treatment, structural alloy steel, structural phase analysis, hardness, microstructure, friction pair, wear

INTRODUCTION

One of the pressing and actively studied problems in the field of mechanical engineering is the improvement of reliability and durability of friction units. Machine components operating in friction pairs under conditions of intensive wear, cyclic loads, and vibrations are subject to special requirements for the wear resistance of the friction surface, while simultaneously ensuring high dynamic strength of the entire product. In this sense, the development of new and the improvement of existing technological methods of surface treatment of materials and machine components appears highly promising. These include various coating methods, ranging from ion-plasma to gas-thermal spraying; methods of alloying, chemical-thermal treatment, or implantation of surface layers with strengthening elements; and different methods of thermomechanical surface treatment, among others. Perhaps one of the most extensively studied directions in strengthening surface layers of different machine parts and assemblies is the treatment of materials with concentrated energy sources (CES) [1–4]. Electron beam, laser energy sources, or plasma jets are predominantly used as CES.

During exposure to concentrated energy sources, the surface is heated followed by cooling due to heat dissipation both into the material and the environment, resulting in structural-phase transformations in the surface layer. The nature of the heating source, heat flux, and exposure time of the surface affect the properties of the thermally strengthened layer (its thickness, physical and mechanical characteristics, phase composition, and dispersion). High-speed heating methods are always characterized by insufficient time for the running and completion of equilibrium structural transformations. Due to changes in the kinetics of phase transformations, grain refinement, and the formation of increased dislocation density under conditions of high-speed heat treatment of the materials, it is possible to obtain the required set of mechanical and physical properties of material surfaces (such as high hardness, wear resistance, corrosion resistance etc.). Heating using CES can be carried out in both continuous and pulsed modes [5]. Compared to conventional heat treatment methods, the pulsed CES heating mode is applied over a very short period (approximately 10^{-3}–10^{-6} s). As a result of intensive heat removal into the metal and the surrounding environment, the cooling time is also several orders of magnitude shorter (10^{-3}–10^{-6} s) than during conventional cooling in liquid quenching media.

In addition, the use of CES proves to be highly effective for carrying out thermal-cyclic treatment of metals and machine components. After such treatment, the surface layer acquires a fine-dispersed structure. It is well known that, at equal hardness, steel with a fine-grained structure has significantly better wear resistance than coarse-grained steel, since the latter demonstrates lower resistance to brittle fracture [6]. As tools for implementing pulsed thermal-cyclic treatment of parts, in addition to laser and electron beam devices, plasma generators

based on powerful pulsed electrical discharges are effectively employed [7, 8]. At the PWI, one variant of such generators was developed and is successfully applied as research equipment both in scientific laboratories [9, 10] and in industrial settings [11].

THE AIM

of this study is to investigate the effect of pulsed plasma treatment (PPT) on structural-phase changes in surface layers and on their wear resistance under lubricated friction conditions.

EQUIPMENT, MATERIALS, AND RESEARCH METHODS

Steel 40Kh (AISI 5140) was selected as the material for investigation. Its chemical composition is as follows, wt.%: C — 0.36–0.44; Si — 0.17–0.37; Mn — 0.50–0.80; Cr — 0.8–1.10, balance — Fe. Steel 40Kh is characterized by increased strength, hardness, and wear resistance. It is widely used across various industrial sectors for manufacturing components and parts operating under high loads, such as shafts, gears, axles, gear wheels, etc. Owing to its mechanical properties, 40Kh steel is also applied in the automotive, mechanical engineering, shipbuilding, and energy industries, where a reliable and durable material is required.

For the study of the structural-phase state of surface layers, a series of samples of steel 40Kh sized 15×15×10 mm was prepared. Tribological experiments were carried out on bushings (Figure 1). A disk with a diameter of 90×10 mm made of ShKh15 steel was used as a counterbody.

The hardness of steel 40Kh in its initial (as annealed) state was measured using the Brinell method and found to be 212–217 *HB*. Before PPT, the samples underwent standard heat treatment. An electric furnace was used for heating, quenching, and tempering. The heating temperature for quenching was 850 °C, which ensured maximum hardness and strength of the material. After soaking in the furnace the samples were quenched in oil, followed by low-temperature tempering at 200 °C for 1 hour.

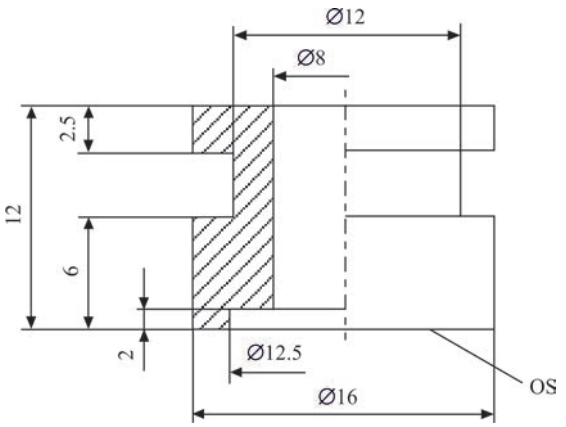

Figure 1. Test sample: bushing (40Kh); WS — working surface

The treatment of the samples was performed using a pulsed plasma generator (Figure 2), characterized by the capability of switching electric current through a partially ionized gas behind the detonation wave front. This enables generation of pulsed plasma with a frequency of 1–4 Hz and energy up to 7 kJ. PPT ensures rapid heating of the surface layer (10^{-3}–10^{-4} s heating time), followed by intensive cooling due to heat removal into the bulk of the product. The high heating and cooling rates (up to 10^7 K/s) promote the formation of fine-dispersed crystalline structures and high dislocation density. The principle of operation and technical parameters of the device are described in [12, 13].

Parameters of pulsed plasma treatment were as follows

Voltage of capacitor bank, kV	3.2
Capacitance of capacitor bank, μF	960
Inductance of discharge circuit, μH	30
Pulse repetition frequency, Hz	2
Distance to treated surface, mm	50
Effective plasma spot diameter on the surface, mm	10
Number of pulses per spot	5
Material of eroded electrode	W

For chemical etching of the microsections under investigation, a 4 % nitric acid (HNO_3) solution was used. Visual analysis of the samples was performed with a Versamet-2 optical microscope. The microstructure of the surface layers was examined using a Quanta 200 3D scanning electron microscope. Mic-

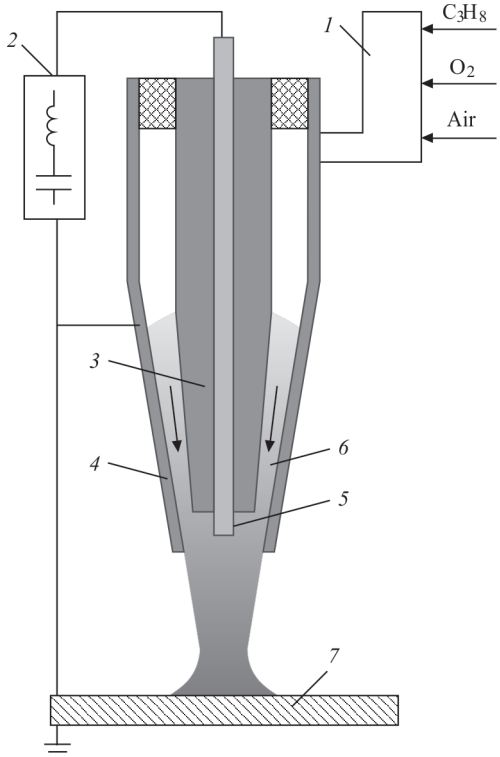

Figure 2. Pulsed plasmatron: *1* — detonation chamber; *2* — power supply; *3*, *4* — coaxial electrodes; *5* — eroded electrode; *6* — plasma; *7* — workpiece

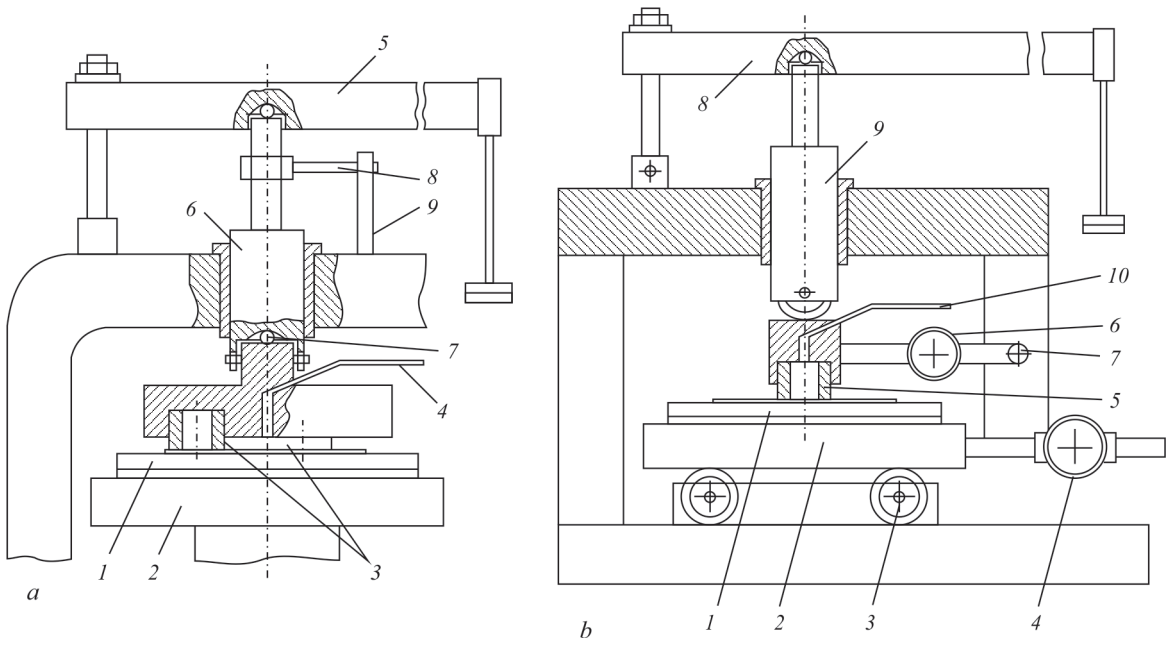

Figure 3. Schemes of the main units of friction machines: *a* — working unit of end friction machine; *b* — working unit of a reverse-friction machine

rohardness was measured in accordance with DSTU ISO 6507-1:2007 on an AFFRI DM8-B microhardness tester using the Vickers method with an indenter load of 50 g. Structural studies were carried out by X-ray diffraction analysis (filming in FeK_α radiation on a DRON-3M diffractometer).

The determination of tribotechnical characteristics of the parts was performed on end and reverse friction machines. Lubrication of the samples in the friction machines was carried out with I-50A type oil and RZh-3 water–oil emulsion, both supplied continuously to the friction zone.

The working unit of the end friction machine is shown in Figure 3, *a*. The moving sample — disk *1* — was mounted on table *2*, which rotates around the vertical axis, driven by the machine. Three stationary samples — bushings *3* — were fixed in a holder and pressed against rotating disk *1* by their end faces. Hose *4* connected to to the holder from a pump supplied lubricant into the friction zone. Lubricant was supplied from a 20 L tank by a pump with a capacity of 3 l/min, and returned to the tank by gravity after passing through the friction zone. The load on the holder with the samples was applied by lever *5* with weights, transmitted through fork *6*. A ball *7* was placed between the fork and the holder to ensure self-alignment of the holder with samples relative to the disk. During holder rotation caused by friction forces, the key of the holder engaged the slot of the fork and turned it. At the upper end of the fork, a rod *8* was rigidly fixed, pressing against a strain gauge *9*. For friction force measurement, the signal from the strain gauge was transmitted to and processed by a weight controller.

The working unit of the reverse friction machine is shown in Figure 3, *b*. The moving sample — disk *1* — was fixed on carriage *2* mounted on four rollers *3*. The carriage was connected via ring *4* to a slider driven by a crank-slider mechanism. The drive of the machine provided adjustable reciprocating motion with a stroke length of 20–70 mm and a double-stroke frequency of 95–320 per minute. The stationary sample — bushing *5* — was fixed in a hole of the holder, which was hingedly attached to shaft *7* through elastic ring *6*. Loading of the samples was achieved by lever *8* with interchangeable weights on its free end. The force was transmitted through rod *9* to the holder with the stationary sample. Lubricant was supplied from a special drop-feed system to the holder via hose *10* at a rate of 3 drops per minute. The friction force was determined using a strain gauge glued to elastic ring *6* and connected to the weight controller.

Wear of the stationary samples (bushings) was evaluated by measuring their mass loss with VLR-200 type analytical balances. Prior to weighing, the samples were washed twice in purified gasoline, then in acetone. After that, the samples were dried in a thermostat at 60 °C for 1 hour. The error in determining the sample mass using this procedure did not exceed 0.0002 g, with the average mass of one bushing being about 7 g.

RESEARCH RESULTS AND DISCUSSION

In 40Kh steel of the pearlitic class, martensite and retained austenite (5–8 vol.%) are formed as a result of quenching. The hardness of the steel after quenching reached 58 *HRC*. During low-temperature tempering (200 °C), tempered martensite is formed due

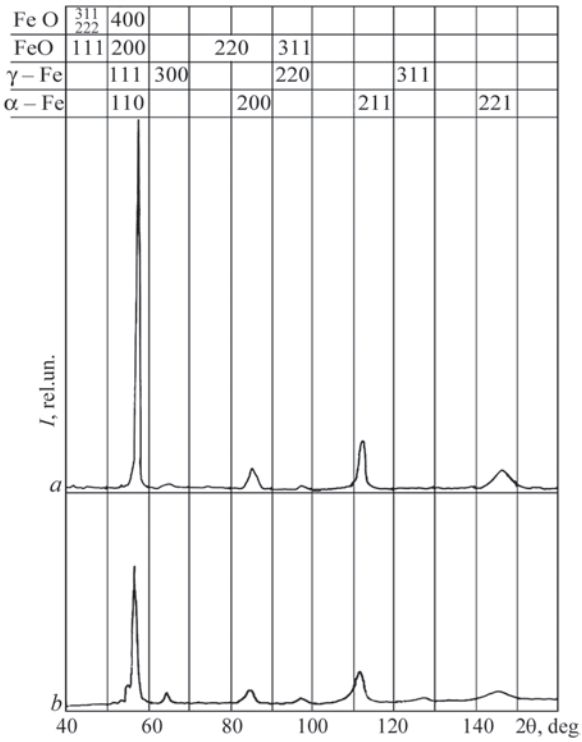

Figure 4. X-ray diffraction pattern of 40Kh steel: *a* — after heat treatment (quenching + tempering); *b* — after pulsed plasma treatment

to the transformation of retained austenite, as well as a decrease in the degree of tetragonality of martensite caused by the release of excess carbon from the α-solid solution. This leads to a slight decrease in hardness to 52 *HRC*.

A typical X-ray diffraction pattern of the sample surface after quenching and low-temperature tempering is shown in Figure 4, *a*. The phase composition of 40Kh steel is mainly tempered martensite with a small amount of retained austenite. PPT of the samples results in significant changes in the structural-phase composition in the surface layers (Figure 4, *b*).

The observed structural changes are consistent with the general concept of surface hardening using SDE (strongly non-equilibrium processes). After PPT, X-ray diffraction shows a broadening of the α-Fe lines and an increase in the intensity of the γ-Fe lines. The main contribution to line broadening comes from lattice defects caused by phase hardening during rapid quenching, as well as carbon inhomogeneity due to the high heating rate and the absence of soaking at high temperature. The broadening of the α-phase lines for this reason is associated with the heterogeneous tetragonality of martensite.

It should also be noted that despite the increase in austenite content (up to 15 vol.%) after PPT, the hardness of the surface layers (as will be shown below) increases due to phase hardening resulting from reversible α↔γ transformations under multiple pulsed impact. The diffraction pattern also shows oxide lines, the slight formation of which on the surface is related to the specifics of PPT. Firstly, oxygen is used as a component of the fuel and, accordingly, of the plasma-forming mixture. Secondly, the treatment is carried out in air.

When examining transverse microsections of the samples after PPT, the formation of a layered structure was revealed. It consists of a weakly etched band up to 35 μm thick (Figure 5) with fine-dispersed martensite of poorly pronounced optical structure, with an integral microhardness of *HV*50 = 8800–10200 MPa (Figure 6). The microhardness of this layer is 1.7 times higher than that of the base metal.

Below the hardened layer, a region up to 25 μm thick with a troostite–martensite structure is formed, where the integral microhardness decreases to *HV*50 ≈ 4500 MPa. In this case, the process of high-speed heating followed by cooling can be considered as a kind of tempering. Deeper, the hardness increases again to the hardness of tempered martensite of the base metal: *HV*50 = 5400–5700 MPa.

Tests of samples with and without PPT were carried out on a pin-on-disc friction machine at sliding speeds of 2, 3.5, and 5 m/s under loads of 0.5, 0.9, and 1.3 MPa. In each mode, the test duration was determined by wear of the samples and it lasted no less than 30 h. The results of tests with industrial oil I-50A and water-oil emulsion RZh-3 supplied into the friction zone are presented in the wear dynamics graphs (Figure 7).

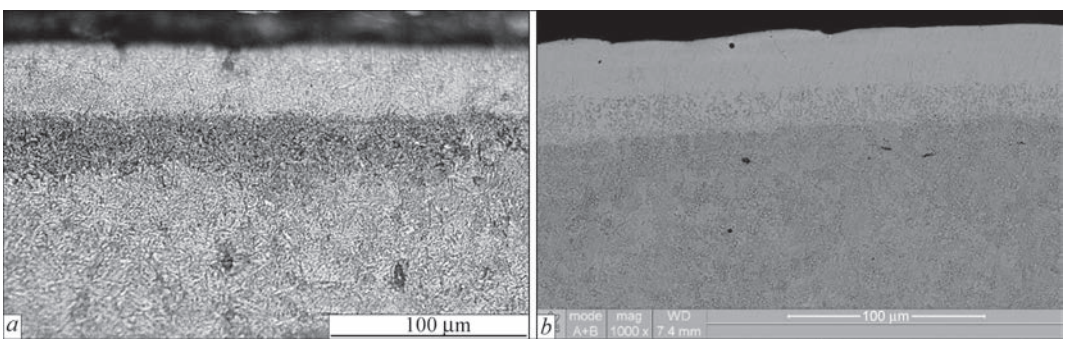

Figure 5. Microstructure of the surface layer of 40Kh steel after pulse-plasma treatment: *a* — image obtained with an optical microscope; *b* — image obtained with a scanning electron microscope

As expected, the use of industrial oil compared to water-oil emulsion significantly reduced the wear process. The minimum wear rate was observed in samples after PPT under all test conditions when using I-50A oil.

When lubricated with both I-50A oil and RZh-3 emulsion, at a constant sliding speed, wear of the samples increased with increasing load. Under fluid friction conditions, increasing the sliding speed contributed to wear reduction, even at higher loads (Figure 7).

Tests of samples on the reverse friction machine were carried out under drop lubrication with emulsion. Test modes were as follows: average sliding speeds were 0.15, 0.3, and 0.45 m/s; loads – 0.5, 0.9, and 1.3 MPa. The test results are presented in the wear dynamics graphs (Figure 8). The influence of sliding speed and load on wear intensity was similar to that observed on the end friction machine. Wear intensity increased with load growth and decreased with increasing sliding speed.

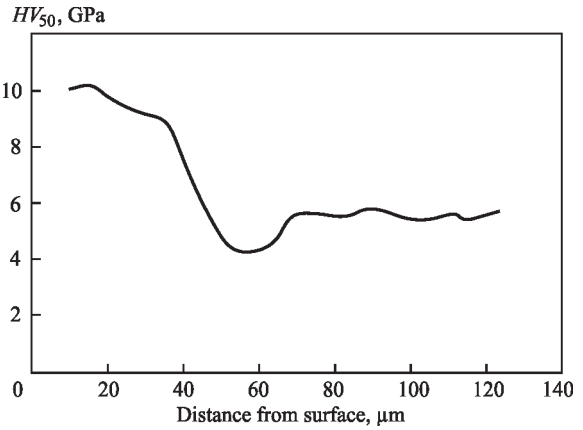

Figure 6. Change in integral microhardness in the surface layers of 40Kh steel after PPT

In most engineering calculations, the friction coefficient is assumed to be constant. However, under real conditions, especially under high loads, it may vary due to changes in contact area, phase transformations, wear, and other factors. Under fluid friction conditions, film thickness varies depending on load, which may also affect the friction coefficient. Studies

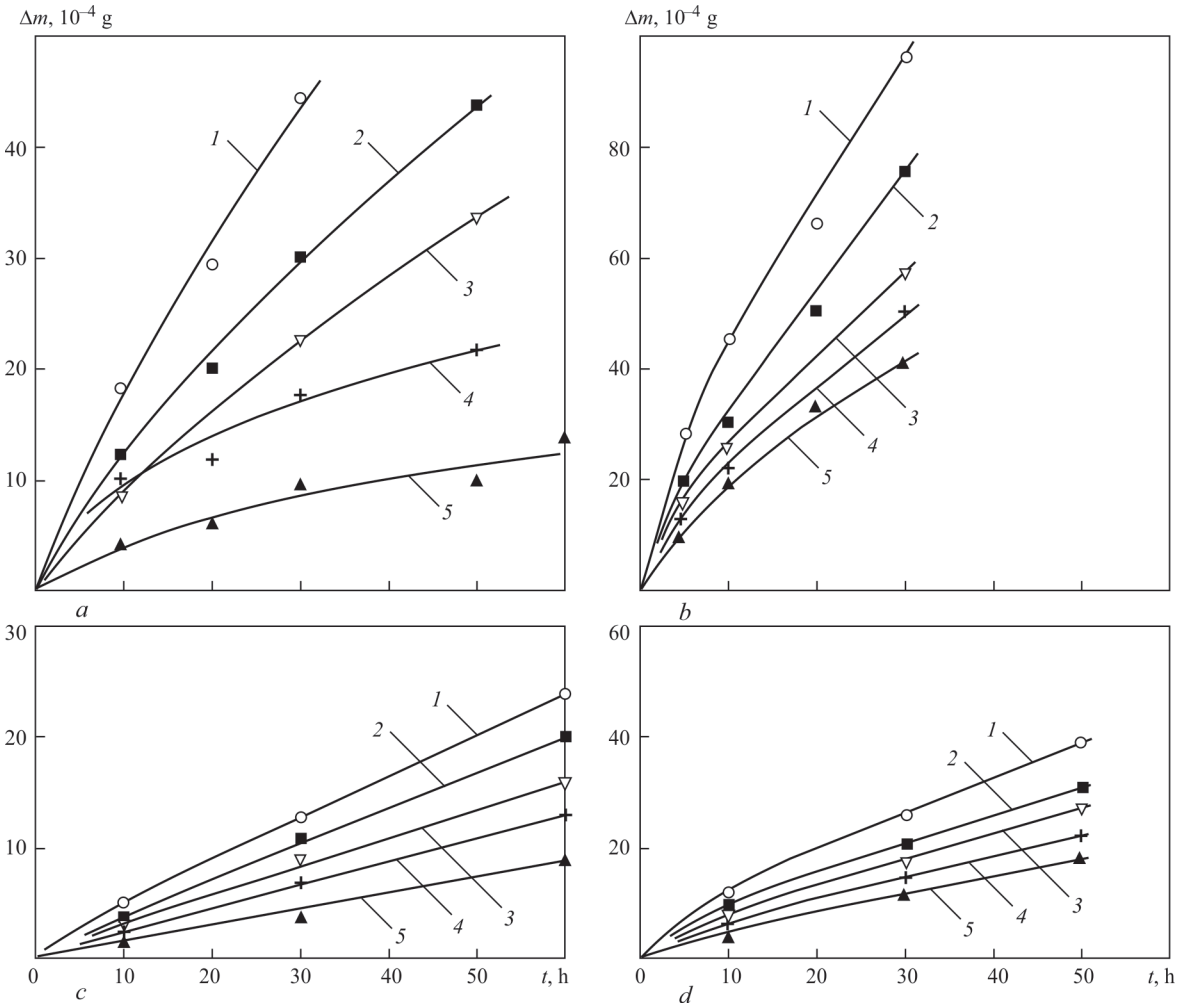

Figure 7. Wear dynamics of bushings on the end friction machine under lubrication: (*a*) with I-50A oil; (*b*) with RZh-3 emulsion; (*a*, *b*) — wear dynamics of bushings without PPT; (*c*, *d*) — wear dynamics of bushings after PPT; *1* — sliding speed 2.0 m/s, load 1.3 MPa; *2* — sliding speed 2.0 m/s, load 0.9 MPa; *3* — sliding speed 3.5 m/s, load 0.9 MPa; *4* — sliding speed 2.0 m/s, load 0.5 MPa; *5* — sliding speed 5.0 m/s, load 0.9 MPa

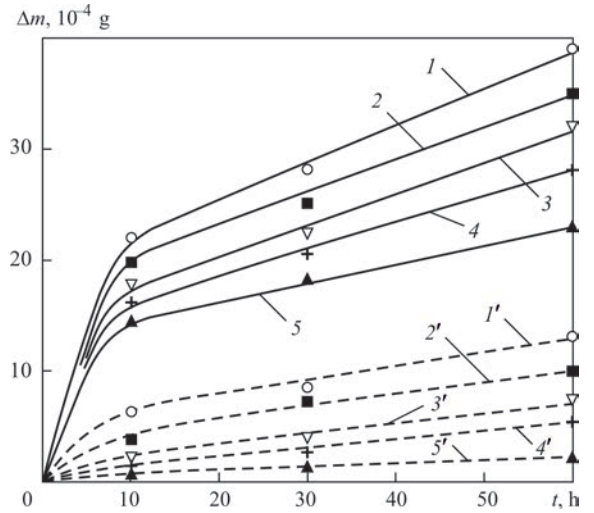

Figure 8. Wear dynamics of parts on a reverse friction machine with RZh-3 emulsion lubrication: a – wear dynamics of bushings; —— parts without PPT; – – – parts after PPT; *1*, *1′* — sliding speed 0.15 m/s, load 0.9 MPa; *2*, *2′* — sliding speed 0.30 m/s, load 0.9 MPa; *3*, *3′* — sliding speed 0.45 m/s, load 1.3 MPa; *4*, *4′* — sliding speed 0.45 m/s, load 0.9 MPa; *5*, *5′* — sliding speed 0.45 m/s, load 0.5 MPa

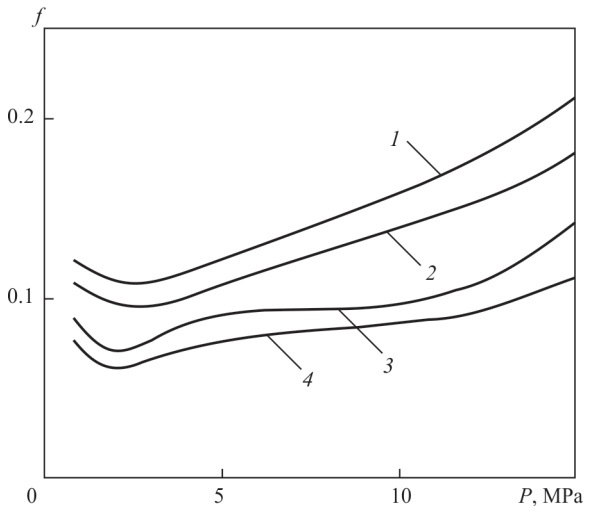

Figure 9. Dependence of the friction coefficient on the load during stepwise loading of samples on a reverse friction machine. Sliding speed 2 m/s. *1* — samples without PPT, friction with emulsion; *2* — samples after PPT, friction with emulsion; *3* — samples without PPT, friction with olive oil; *4* — samples after PPT, friction with olive oil

on both the end and reverse friction machines showed that the fluid friction coefficient changed little during testing. For samples without PPT on the end friction machine, depending on run-in time and test mode, the coefficient ranged from 0.07 to 0.12 and 0.1 to 0.13 when lubricated with I-50A and RZh-3, respectively. PPT reduced the friction coefficient by an average of 0.015. On the reverse friction machine under drop lubrication with emulsion and at the above test conditions, the friction coefficient for untreated and treated pairs was 0.12–0.16 and 0.1–0.14, respectively.

After prolonged testing of samples on the reverse friction machine at a speed of 2 m/s and a load of 1.3 MPa, burr tests were carried out on run-in samples (Figure 9). During the experiment, the load on the friction pair was stepwise increased by 1 MPa. At each stage, the pair operated for 10 minutes, after which the friction force was recorded, and the load was increased. A maximum load of 15 MPa was reached, but further load increase was not possible due to machine design limitations. As a result, burring could not be achieved.

CONCLUSIONS

1. Using the method of X-ray structural phase analysis, it was shown that after surface PPT of 40Kh steel samples, a hardened surface layer is formed, consisting of fine-dispersed martensite, retained austenite (14.8 vol.%), as well as a small amount of oxides. The increase in retained austenite at high cooling rates (up to 10^7 K/s) is associated with the suppression of high-temperature austenite decomposition during high-speed martensitic transformation.

2. Multiple thermal impact of pulse plasma enables the implementation of surface thermocyclic treatment, which contributes to the enhancement of phase hardening due to reversible α↔γ transformations, an increase in dislocation density, and grain refinement. As a result, a surface layer with a thickness of 35 μm is formed, exhibiting increased microhardness — *HV*50 = 8800–10200 MPa, which is 1.7 times higher than the microhardness of the base metal.

3. Analysis of the presented experiments shows that the tribological properties of the samples under fluid friction conditions are significantly improved as a result of their strengthening by the pulse plasma method. In particular, the strengthening provides a reduction in the wear rate of the samples by 1.2–3.7 times when lubricated with oil and by 1.4–4.3 times when lubricated with emulsion during tests on an end friction machine, and by 1.8–3 times on a reverse friction machine when lubricated with emulsion. In all cases, the strengthening ensures a reduction in the fluid friction coefficient by 0.01–0.02.

REFERENCES

1. Dinesh Babu, P., Balasubramanian, K.R., Buvanashekaran, G. (2011) Laser surface hardening: A review. *Inter. J. of Surface Sci. and Eng.*, 5(**2–3**), 131–151. DOI: https://doi.org/10.1504/IJSURFSE.2011.041398
2. Kwok, C.T., Man, H.C., Cheng, F.T., Lo, K.H. (2016) Developments in laser-based surface engineering processes: with particular reference to protection against cavitation erosion. *Surface and Coatings Technology*, **291**, 189–204. DOI: https://doi.org/10.1016/j.surfcoat.2016.02.019
3. Zou, J.X., Zhang, K.M., Hao, S.Z. et al. (2010) Mechanisms of hardening, wear and corrosion improvement of 316 L stainless steel by low energy high current pulsed electron beam surface treatment. *Thin Solid Films*, 519(**4**), 1404–1415. DOI: https://doi.org/10.1016/j.tsf.2010.09.022

4. Lashchenko, G.I. (2003) *Plasma hardening and spraying*. Kyiv, Ekotechnologiya [in Russian].
5. Maharjan, N., Zhou, W., Zhou, Y. et al. (2019) Comparative study of laser surface hardening of 50CrMo4 steel using continuous-wave laser and pulsed lasers with ms, ns, ps and fs pulse duration. *Surface and Coatings Technology*, **366**, 311–320. DOI: https://doi.org/10.1016/j.surfcoat.2019.03.036
6. Fedyukin, V.K., Smagorinsky, M.E. (1989) *Thermocyclic processing of metals and parts*. Leningrad, Mashinostroenie [in Russian].
7. Minko, L.Ya. (1970) *Generation and study of pulsed plasma flows*. Minsk, Nauka i Tekhnika [in Russian].
8. Chabak, Y.G., Fedun, V.I., Pastukhova, T.V. et al. (2017) Modification of steel surface by pulsed plasma heating. *Probl. At. Sci. Technol.*, **110**, 97–102. https://vant.kipt.kharkov.ua/ARTICLE/VANT_2017_4/article_2017_4_97.pdf
9. Yu, J., Zhang, L., Liu, K. et al. (2017) Effect of pulse detonation-plasma technology treatment on T8 steel microstructures. *J. of Materials Eng. and Performance*, **26**, 6198–6206. DOI: https://doi.org/10.1007/s11665-017-3067-y
10. Özbek, Y.Y. (2020) Surface properties of AISI 4140 steel modified by pulse plasma technique. *J. of Materials Research and Technology*, 9(**2**), 2176–2185. DOI: https://doi.org/10.1016/j.jmrt.2019.12.048
11. Tyurin, Yu.N., Kolisnichenko, O.V., Tsygankov, N.G. (2001) Pulse-plasma hardening of tools. *The Paton Welding J.*, **1**, 38–44.
12. Korzhyk, V., Tyurin, Y., Kolisnichenko, O. (2021) *Theory and practice of plasma-detonation technology of surface hardening metal products*. Kharkiv, PC Technology Center. DOI: https://doi.org/10.15587/978-617-7319-46-6
13. Tyurin, Y.N., Kolisnichenko, O.V. (2009) Plasma-detonation technology for modification of the surface layer of metal parts. *Open Surface Sci. J.*, **1**, 13–19. DOI: http://dx.doi.org/10.2174/1876531900901010013

ORCID
O.V. Kolisnichenko: 0000-0003-4507-9050,
V.M. Korzhyk: 0000-0001-9106-8593,
C. Senderowski: 0000-0002-0331-3702,
D.V. Strogonov: 0000-0003-4194-764X,
O.V. Hanushchak: 0000-0003-4392-6682,
O.S. Tereshchenko: 0009-0003-4021-0758

CONFLICT OF INTEREST
The Authors declare no conflict of interest

CORRESPONDING AUTHOR
O.V. Kolisnichenko
E.O. Paton Electric Welding Institute of the NASU
11 Kazymyr Malevych Str., 03150, Kyiv, Ukraine.
E-mail: okolis@i.ua

SUGGESTED CITATION
O.V. Kolisnichenko, V.M. Korzhyk, C. Senderowski, D.V. Strogonov, O.V. Hanushchak, O.S. Tereshchenko (2025) Influence of pulse plasma treatment on wear resistance of 40Kh steel surface layers. *The Paton Welding J.*, **9**, 39–45.
DOI: https://doi.org/10.37434/tpwj2025.09.05

JOURNAL HOME PAGE
https://patonpublishinghouse.com/eng/journals/tpwj

Received: 18.04.2025
Received in revised form: 19.06.2025
Accepted: 24.09.2025